

Hydrological mobilization of mercury and dissolved organic carbon in a snow-dominated, forested watershed: Conceptualization and modeling

J. Schelker,¹ D. A. Burns,² M. Weiler,³ and H. Laudon¹

Received 16 February 2010; revised 7 September 2010; accepted 14 September 2010; published 12 January 2011.

[1] The mobilization of mercury and dissolved organic carbon (DOC) during snowmelt often accounts for a major fraction of the annual loads. We studied the role of hydrological connectivity of riparian wetlands and upland/wetland transition zones to surface waters on the mobilization of Hg and DOC in Fishing Brook, a headwater of the Adirondack Mountains, New York. Stream water total mercury (THg) concentrations varied strongly (mean = $2.25 \pm 0.5 \text{ ng L}^{-1}$), and the two snowmelt seasons contributed 40% (2007) and 48% (2008) of the annual load. Methyl mercury (MeHg) concentrations ranged up to 0.26 ng L^{-1} , and showed an inverse log relationship with discharge. TOPMODEL-simulated saturated area corresponded well with wetland areas, and the application of a flow algorithm based elevation-above-creek approach suggests that most wetlands become well connected during high flow. The dynamics of simulated saturated area and soil storage deficit were able to explain a large part of the variation of THg concentrations ($r^2 = 0.53$ to 0.72). In contrast, the simulations were not able to explain DOC variations and DOC and THg concentrations were not correlated. These results indicate that all three constituents, THg, MeHg, and DOC, follow different patterns at the outlet: (1) the mobilization of THg is primarily controlled by the saturation state of the catchment, (2) the dilution of MeHg suggests flushing from a supply limited pool, and (3) DOC dynamics follow a pattern different from THg dynamics, which likely results from differing gain and/or loss processes for THg and/or DOC within the Fishing Brook catchment.

Citation: Schelker, J., D. A. Burns, M. Weiler, and H. Laudon (2011), Hydrological mobilization of mercury and dissolved organic carbon in a snow-dominated, forested watershed: Conceptualization and modeling, *J. Geophys. Res.*, *116*, G01002, doi:10.1029/2010JG001330.

1. Introduction

[2] Anthropogenic emissions of mercury (Hg) to the atmosphere have increased the actively cycled pool of mercury by threefold to fivefold, and Hg contamination of aquatic ecosystems in the United States and across the globe is widespread [Lindberg *et al.*, 2007; Munthe *et al.*, 2007]. Methylmercury (MeHg) is of particular concern because this form bioaccumulates and biomagnifies in aquatic and terrestrial food webs, and as a result, Hg fish consumption advisories have been listed for surface waters in all 50 U.S. states [U.S. Environmental Protection Agency (EPA), 2009]. The source of Hg to most catchments is believed to be atmospheric deposition that originates from human and natural emissions of which coal burning is the leading source

[Pacyna *et al.*, 2006]. In northeastern North America, atmospheric Hg deposition appears to be decreasing in recent years [Butler *et al.*, 2008], but Hg in lake sediment cores has not yet shown widespread and universal declines [Muir *et al.*, 2009]. Annual loads of Hg exported from catchments, however, are generally only a small fraction of annual deposition, and even when gaseous losses are estimated, many sites continue to be net accumulators of Hg [Shanley *et al.*, 2008; Brigham *et al.*, 2009].

[3] Soils are the largest store of Hg in most catchments and typically the mineral soil has a greater store of Hg than the forest floor despite higher Hg concentrations per unit of soil mass in the organic horizons [Grigal, 2003]. Even higher Hg concentrations are observed in wetlands and in peaty soils, and this Hg is believed to be largely associated with soil organic carbon, suggesting that organic carbon distribution in a catchment landscape controls Hg distribution [Grigal, 2003]. Concentrations of THg and MeHg vary greatly among surface waters, and this spatial variation typically exceeds the spatial variations in atmospheric Hg deposition [Wiener *et al.*, 2006]. Wetlands are believed to be one of the key landscape features that affect Hg storage and transport, and percent wetland area is often strongly related to surface

¹Department of Forest Ecology and Management, Swedish University of Agricultural Sciences, Umeå, Sweden.

²Watersheds Research Section, U.S. Geological Survey, Troy, New York, USA.

³Institute of Hydrology, Albert-Ludwigs-Universität Freiburg, Freiburg, Germany.

water Hg concentrations [Brigham *et al.*, 2009]. Despite the importance of wetlands to Hg transport, wetland area is sometimes unrelated to Hg concentrations in adjacent waters, which highlights the pivotal role that the hydrologic connection of wetlands with local waters can play in the catchment Hg cycle [Selvendiran *et al.*, 2008]. Other landscape factors are known to affect the Hg cycle in catchments such as the presence of forests, the relative amount of coniferous forest, and the hydrologic connection of upland and wetland or riparian areas [Kolka *et al.*, 2001; Choi *et al.*, 2008; Mitchell *et al.*, 2008b].

[4] Wetlands generally act as net sinks of inorganic Hg [Kolka *et al.*, 2001], and these losses are assumed to be largely through sorption processes. Although Hg in the elemental form (Hg^0) can readily exchange as a gas into and out of soils [Choi and Holsen, 2009], most wetlands are likely accumulating ionic Hg, particularly those with peaty soils [Klaminder *et al.*, 2008]. Some of the Hg pool can become methylated by bacteria under anaerobic conditions; this process is generally believed to be carried out largely by sulfate reducing bacteria (SRB) [Benoit *et al.*, 2003; Drott *et al.*, 2007] for which the availability of sulfate and labile DOC are often controlling factors [Mitchell *et al.*, 2008a]. Additional losses of Hg within catchments can occur by photoreduction of Hg and volatilization of the resulting Hg^0 , directly from surface waters, and MeHg can be removed through biological and physical demethylation processes in streams and ponds [Krabbenhoft *et al.*, 2005].

[5] The transport of Hg between upland areas and riparian areas is often favored by the flux of water between these two landscape features [Selvendiran *et al.*, 2009]. Rapid runoff from uplands can speed the transport of Hg to wetlands, where methylation may occur [Kolka *et al.*, 2001]. The loads of Hg and DOC that reach the outlet of a catchment may be less dependent on the amount of Hg stored in the soils, than on the efficiency of physical and chemical mobilization processes [Demers *et al.*, 2010].

[6] Numerous studies show strong positive relationships between total mercury and DOC or particulate organic carbon (POC) concentrations in stream water [Driscoll *et al.*, 1995; Schuster *et al.*, 2008; Selvendiran *et al.*, 2008; Dittman *et al.*, 2010], which reflects the dependence of Hg(II) on binding to soluble organic matter to facilitate transport [Haitzer *et al.*, 2002; Dittman *et al.*, 2010]. Furthermore, the hydrophobic organic acid fraction (HPOA) of DOC has been found to explain a higher fraction of the variability of Hg concentrations in surface waters than can be explained by DOC concentrations [Shanley *et al.*, 2008; Dittman *et al.*, 2009].

[7] The mobilization of Hg from soils is driven in large part by changing hydrological conditions, especially high-flow events such as the observed direct responses of THg concentrations in stream water to rain storms and snowmelt events [Bishop *et al.*, 1995; Shanley *et al.*, 2002; Bushey *et al.*, 2008; Schuster *et al.*, 2008; Demers *et al.*, 2010; Dittman *et al.*, 2010].

[8] New conceptualizations of the flushing of mercury and DOC caused by changing flowpaths in soils as well as changing source areas [Demers *et al.*, 2010; Dittman *et al.*, 2010], often represented by the strong coupling of DOC and THg concentrations [Dittman *et al.*, 2009], suggest the possibility of developing joint conceptualizations for both of these constituents. Numerous model applications have been

applied to investigate the process of hydrological DOC mobilization to surface waters through chemical mixing models [Brown *et al.*, 1999; Christophersen and Hooper, 1992; van Verseveld *et al.*, 2008] and rainfall-runoff models [Hornberger *et al.*, 1994; Boyer *et al.*, 1997; Weiler and McDonnell, 2006], often referred to as a “flushing mechanism” [Burns, 2005]. Whereas initial attempts to conceptualize hydrologic processes of Hg mobilization through the application of simple mixing models in small watersheds have shown some potential [e.g., Demers *et al.*, 2010], little has been done to conceptualize landscape-scale hydrologic processes of Hg mobilization by the application of spatially explicit hydrologic models in larger and more complex watersheds.

[9] Recent research in the Adirondack Mountains of New York indicates that the connection of small riparian wetlands to major hydrologic flow paths provide important controls on THg, MeHg and DOC in streams [Inamdar and Mitchell, 2006; Selvendiran *et al.*, 2008]. We assume that similar processes would also operate at a catchment scale that is greater than that of the above mentioned studies, and hypothesize that the riparian area in small upland tributary streams, and the wetland/upland interface in higher-order stream channels represent major landscape controls on DOC and Hg species. Further we hypothesize that high-flow conditions will increase the connectivity of upland areas to riparian wetlands that dominate in lower valley bottoms and mobilize Hg and DOC from surface soil layers. Therefore, the aim of this study was to investigate the role of hydrological controls on the mobilization of THg, MeHg and DOC during high-flow conditions in the Fishing Brook (FB) Catchment, Adirondack Mountains, New York State. A combined field and modeling approach was used, based on saturation state simulations with the hydrological model TOPMODEL [Beven and Kirkby, 1979; Ambroise *et al.*, 1996; Ibbitt *et al.*, 2009] to identify first-order controls on the mobilization of Hg and DOC. We define the following terms for use in this study: (1) “hydrological flushing” as the process of transport of Hg or DOC from the terrestrial to the aquatic system and (2) “net mobilization” as the combination of a flushing process and additional processes within the stream network which may alter Hg and DOC concentrations prior to sampling at the catchment outlet.

2. Study Site

2.1. General Description

[10] Fishing Brook is a 65 km² catchment (Figure 1) in the headwaters of the Hudson River basin, in the central part of the Adirondack State Park in northern New York (43°58'31"N, 74°20'04"W). The outlet of the catchment is located at the downstream end of a pond named County Line Flow (CLF). The morphology of the catchment is mainly characterized by the strong influence of glacial epochs. The landscape is moderately mountainous with large riparian wetland areas in the valley bottoms. The elevation ranges from 502 to 1082 m and the landscape can be divided into three distinctive landscape features: upland areas, wetlands and open water bodies (i.e., lakes and ponds). The catchment area consists of 89% uplands, 8% wetlands, and 3% open water (Figure 1).

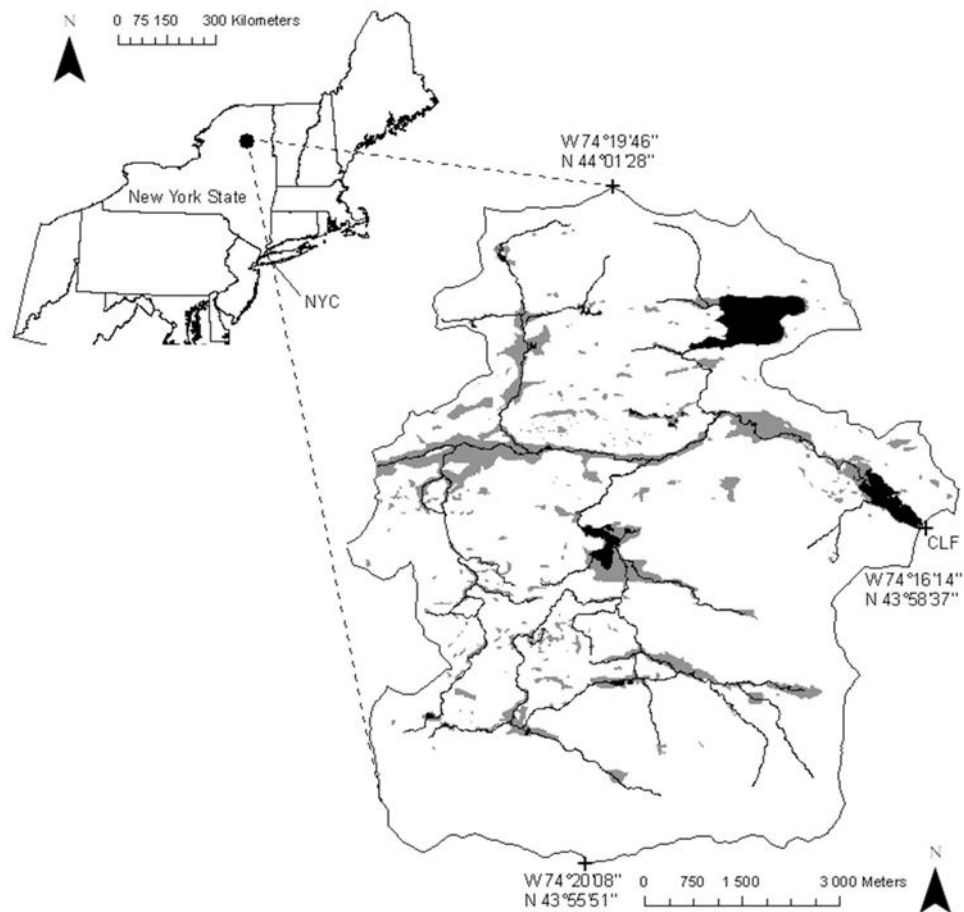


Figure 1. Fishing Brook Catchment in the Adirondack State Park, New York State. Shown are the stream network (solid black lines), open water bodies (solid black), and wetlands (gray).

[11] The climate is a typical cool and moist northern continental climate. The annual mean temperature (1951–1980) at Huntington Wildlife Forest 3.9 km northeast of study site is 4.4°C, the January mean is −10.2°C, and the July mean 17.4°C [Shepard *et al.*, 1989]; average annual precipitation is 1010 mm yr⁻¹, of which 47% falls as snow.

[12] Vegetation is predominantly mixed northern hardwoods, consisting of American beech (*Fagus grandifolia*), sugar maple (*Acer saccharum*), and yellow birch (*Betula alleghaniensis*) in upland areas. Wetland vegetation is dominated by red spruce (*Picea rubens*) and balsam fir (*Abies balsamea*) in forested wetland areas, which account for 36% of the wetland area and speckled alder (*Alnus incana*) and various sedges (*Carex*) in lower wetlands which are covered by shrub type vegetation and represent 38% of the total wetland area [Mitchell *et al.*, 2001; Selvendiran *et al.*, 2008; APA wetland data set].

[13] The FB Catchment is located within a Precambrian Anorthosite Massif in the central Adirondack Mountains. This large igneous intrusion has high amounts of calcium-rich feldspar [Mitchell *et al.*, 2001] which preferentially dissolves as the rock weathers. These rocks are mainly granitic gneiss with some gabbro-amphibolite from the synenite-granite series [Fischer, 1957]. The surficial geology is dominated by sandy glacial till which was deposited at the end of the Wisconsinan Glacial Epoch [Mitchell *et al.*, 2001].

Sand and till layers are often present between the mineral soil and the underlying bedrock [McHale *et al.*, 2000]. Valley bottom riparian areas are dominated by a combination of glacial and postglacial alluvial outwash containing sand and gravel with isolated areas of peat overlying sandy soils. Upland areas are generally coarse loamy Spodosols.

2.2. Hydrology

[14] The FB catchment is characterized by a fairly rapid response to rainfall and snowmelt. Peakflow was typically reached within 9–12 h after the onset of distinct rain or snowmelt events, but is slowed during recession by the abundant flat valley bottoms containing wetlands and ponds. On hillslopes, a shift from subsurface flow to surface runoff was observed as overland flow in several locations between the unfrozen soil surface and the snowpack during snowmelt. Additionally we observed overland flow in some steeper, forested locations with high infiltration capacities; a process, sometimes referred to as “organic layer interflow” [Weiler and McDonnell, 2004], which does not necessarily require infiltration excess at the soil surface on hillslopes (see also auxiliary material).¹

¹Auxiliary materials are available in the HTML. doi:10.1029/2010JG001330.

[15] In the valley bottoms, two different processes were observed. First, the water table rose rapidly to the soil surface, flooding the riparian wetlands, and thereby enlarging the direct contribution of channel precipitation to discharge during rain events. Second, when the water table reached the surface, or when riparian areas were flooded by stream water, the melting of snow was greatly enhanced, providing a higher direct runoff contribution during periods of high snowmelt. Return flow [Brown *et al.*, 1999] was also observed in the field at the upland/wetland interface, where water emanated at abrupt changes of slope and seasonal groundwater springs that drain the highly conductive sand layers. Similar springs were also identified by Burns *et al.* [1998] in the Catskill Mountains of NY and by McHale *et al.* [2002] in the nearby Archer Creek Watershed.

3. Methods

3.1. Field Sampling, Lab Analysis, and Statistical Calculations

[16] At the catchment outlet, CLF, discharge was computed on an hourly basis from water level measurements at an H weir located below a bridge at the outlet of a shallow pond. Winter measurements showed little disturbance by ice formation due to high-flow velocities.

[17] Water samples were collected on a monthly basis with additional samples taken during high-flow conditions such as snowmelt and rain storms by wading into the stream to the approximate centroid of flow and dipping media bottles to the approximate midpoint between the water and sediment surface. Two bottles were used for each of THg (2 L) and MeHg (1 L) analysis, and were new, factory-sealed and consisted of Nalgene polyethylene terephthalate copolyester (PETG). A glass bottle was used for sample collection for DOC and Abs₂₅₄ analysis. Each sample bottle was rinsed three times with stream water prior to collecting the sample. A clean-sampling technique similar to the U.S. Environmental Protection Agency (EPA) Method 1669 was used that employed shoulder-length polyethylene gloves and wrist-length nitrile gloves during field sampling [EPA, 1996].

[18] Water samples were filtered first and then preserved, usually both within a few hours of collection. Filtered total Hg (FTHg) and methyl Hg (FMeHg) were determined from samples that were vacuum-filtered through a 0.7 μm pore size, prebaked (550°C) quartz-fiber filter. Aliquots were then acidified to approximately 1% with HCl in the field and stored in the dark until analysis. Particulate total mercury (PTHg) and methylmercury (PMeHg) were determined from the aforementioned quartz fiber filters, which were placed on dry ice immediately after filtration and were stored frozen until analysis. Samples for DOC and Abs₂₅₄ analysis were pressure-filtered with baked glass fiber filters into 40 mL (mL) amber glass vials and stored at 4°C until analysis.

[19] Mercury analyses were conducted at the USGS Wisconsin Mercury Research Laboratory. FTHg was determined by cold vapor atomic fluorescence spectrometry (CVAFS) according to a method described by Olson and DeWild [1999]. FMeHg was determined after distillation by ethylation, gas chromatographic separation, pyrolysis, and CVAFS as described by DeWild *et al.* [2002]. PTHg was analyzed by digesting quartz fiber filters with aqua regia,

treating with bromine monochloride, and then analysis by a method similar to that for FTHg [Olund *et al.*, 2004]. PMeHg was analyzed by treating quartz fiber filters with potassium bromide, copper sulfate, and methylene chloride. An aliquot of reacted methylene chloride was transferred to water and the sample was then treated similarly to water samples [DeWild *et al.*, 2004]. Matrix spikes for analytical runs that included the samples discussed in this paper yielded a mean recovery of 99% (SD = 7%) for FTHg, and 97% (SD = 22%) for FMeHg. THg is the sum of FTHg and PTHg, and MeHg is the sum of FMeHg and PMeHg. DOC concentrations were determined by a persulfate wet oxidation method and Abs₂₅₄ was measured in a spectrophotometer at a wavelength of 254 nm.

[20] Quality control was evaluated through collection of replicate samples and processing of field blank samples. Four field blank samples which were handled and processed similar to regular stream samples were analyzed during the 17 month study period. The mean blank value for FTHg was 0.05 ng/L and no values exceeded 0.08 ng/L. Three of four blanks for PTHg were below the method detection limit (variable, but usually about 0.09 ng/L), and one had a value of 0.1 ng/L. All blank samples were below the method detection limit for FMeHg (0.04 ng/L) and PMeHg (0.01 ng/L). The mean value for blanks analyzed for DOC was 0.6 mg/L, and all values were less than 0.9 mg/L, and for Abs₂₅₄, all blanks had a value of 0.001. Four replicate samples were collected from FB, and the mean standard deviation of these replicates was 0.17 ng/L for PTHg and 0.03 ng/L for FMeHg. Comparable values for PTHg and PMeHg were 0.04 ng/L and 0.01 ng/L, respectively. Further, samples with visible color were exposed to UV radiation prior to analysis to eliminate possible matrix interference from DOC. Five replicate samples were analyzed for DOC and Abs₂₅₄, and the mean standard deviation of these values were 0.34 mg/L and 0.008, respectively. THg and MeHg concentrations which were reported as below the detection limit (0.04 ng L⁻¹, determined by filtered fractions) were set to half the concentration of the minimum detectable concentration (0.02 ng L⁻¹) for data analysis.

[21] Additionally, in situ measurements of pH, dissolved oxygen, and water and air temperature were performed at the time of sampling using a Hydrolab Surveyor handheld equipped with a MS-5 sonde which was recalibrated before every use.

[22] To investigate the role of the pond at the outlet of FB (CLF) additional samples were collected just upstream of CLF as well as at the stream gage at the downstream end of the pond on six dates during the 2007 (May, August, and October) and 2008 (May, July, and October) growing seasons. Additionally, two first-order tributaries were sampled on six (principal tributary to County Line Flow) and four (principal tributary to Pickwacket Pond) occasions during May 2007 to October 2008. Samples were generally collected within 48 h at all sites during a sample period with slowly receding low-flow conditions (flow variation was <10% at gage during all sampling periods). The upstream sampling location drains an area equivalent to 92% of that of the gage at CLF. Discharge of the County Line Flow tributary was measured with a current meter at the time of each sample collection, and the mean value was equivalent to 11% of that at the gage, confirming

that this stream was the principal inflow to CLF, and suggesting little additional groundwater or tributary discharge to the Flow. Two types of groundwater samples were collected in the Six Mile Brook catchment, a tributary to FB, (1) seeps, and (2) piezometers. These samples were collected from a broad riparian wetland area classified as scrub-shrub, and with sandy soils rich in organic matter as is typical of the Wonsqueak-Rumney-Bucksport Complex, which underlie this wetland type within FB. The seeps were shallow channeled rivulets in the wetland that discharged directly to the stream. Up to seven different seeps were sampled in the riparian wetland on each of six dates during October 2007 to October 2009. The seeps were filtered in the lab using the same procedure and filters described previously for surface waters. Seeps were sampled by placing collection bottles into the center of the rivulet with the mouth pointing upstream similar to stream water collections. Particulate Hg was not measured in these seeps because small amounts of bottom sediment were sometimes disturbed during sampling and observed to enter the bottle.

[23] The piezometers consisted of 38 mm ID, Schedule 40 PVC pipe with a screen length of 300 mm. Piezometers were installed such that the top of the screen was at a depth of 150 mm, resulting in a sampling depth interval of 150 to 450 mm. Fifteen piezometers were located at variable distances of about 1 to 50 m from the stream, and on both sides of the channel along a reach of about 600 m in length. The piezometers were sampled by removing one well volume of water with a peristaltic pump and returning to collect a sample with the same pump once the water level recovered to its previous depth. Piezometers were filtered in the field on a mobile table using the same setup as in the lab, but with filter chambers placed inside a plastic bag that served as a glove box to prevent contamination from windborne dust. All tubing that contacted the well and groundwater was of fluoropolymer composition and cleaned, dried, and bagged according to procedures recommended by *Lewis and Brigham* [2004]. Particulate Hg was not measured in the piezometer samples because of the disturbance that resulted from pumping.

[24] Load and yield calculations were based on daily mean discharge values derived from the hourly data and linear interpolation of concentrations for the between-sampling time interval. Loads are reported in mass units, and yields are reported as a mass per unit catchment area per unit time.

[25] For some analyses in this paper, we have distinguished snowmelt as well as the growing and nongrowing seasons as follows: (1) 2007 snowmelt was 8 March 2007 to 22 May 2007 and 2008 snowmelt was 25 March 2008 to 4 May 2008, and (2) growing seasons were 23 May 2007 to 31 October 2007 and 5 May 2008 to 31 October 2008. The 1 year period used for load calculations is defined as 12 June 2007 to 11 June 2008 which includes the 2007 snowmelt.

[26] Linear regressions were calculated with Sigmaplot 11.0 (Systat Software, Inc.) or SPSS 17.0 (IBM Inc.). Correlations were considered if the tests for normality (Shapiro-Wilk) and constant variance were passed. Linear regressions are reported as significant if $p < 0.05$ and highly significant if $p < 0.001$, with p being the significance level for either the slope or the y intercept. If linear regression models were differentiated by season, differences between regres-

sions were tested for significance and are shown if $p < 0.05$ for either the slope or the y intercept.

3.2. Modeling

3.2.1. TOPMODEL

[27] To represent the hydrologic dynamics of areas in the catchment that become temporarily saturated, the rainfall/runoff model TOPMODEL [*Beven and Kirkby*, 1979] was applied. This model combines a simple lumped parameter concept with the idea of streamflow generation by 'variable contributing areas' [*Wolock*, 1993] which, following our hypothesis, tend to be flat, riparian areas that are frequently covered by wetlands, and extend to the interface with upland areas; and, thus, are the major controls of Hg mobilization. The model considers topographic and soil properties by simulating the response of the catchment based on the topographic wetness index TWI ($\ln(m)$) as defined in formula 1:

$$TWI = \ln\left(\frac{a}{\tan\beta}\right) \quad (1)$$

where a is the upslope accumulated area, and β is the slope.

[28] The main routine of TOPMODEL used in this study is similar to the formulation described by *Wolock* [1993]. Model parameterization was based on the most sensitive parameters, which were identified from test simulations and from the results of earlier studies (*D. Wolock*, personal communication, 2010). Model performance was evaluated by the N_{eff} objective function (equation (2)) as given by *Nash and Sutcliffe* [1970].

$$N_{eff} = 1 - \frac{\sum_t (Q_{obs}(t) - Q_{sim}(t))^2}{\sum_t (Q_{obs}(t) - \bar{Q}_{obs})^2} \quad (2)$$

where Q_{obs} is the observed and Q_{sim} the simulated discharge at time step t , respectively. This measure describes the model performance as a better predictor of flow than using the mean value if $N_{eff} > 0$, with a perfect model fit resulting in a N_{eff} of 1. The fitting was performed by applying 10,000 Monte-Carlo simulations for the 6 most sensitive parameters which were assumed to follow a uniform probability distribution within the given range. Besides the parameters which were used to fit the model, general catchment properties were specified as lumped parameters. Table 1 shows the parameter ranges used for the Monte-Carlo simulations as well as an overview of all catchment characteristics represented as lumped parameters.

[29] TOPMODEL simulations were performed on a daily time step. The input file containing mean daily air temperature, daily precipitation and measured discharge was generated from climate data from the nearby climate station in Newcomb, NY as well as from aggregating daily values from the gaging station. The calibration was performed for 1 January 2006 to 16 June 2008. Because the stream gage at FB was installed in January 2007, discharge data for the first year used for model calibration were derived by applying a forward stepwise regression model to discharge data from surrounding gauging stations. The best model fit was reached with data from the following five stations: three USGS gages at Hudson River near Newcomb, NY (USGS ID number 01312000), Ausable River near Au Sable Forks, NY

Table 1. Static Model Parameters and Parameter Ranges Used for the Model Calibration With the Monte-Carlo Method^a

	Description	Unit	Value or Range	Best ₁	Best ₁₀	SD
K_D	Saturated hydraulic conductivity of C horizon	(mm h ⁻¹)	5–3810	3327.4	2580.6	(±851.6)
K_{mult}	Difference in permeability between top and bottom of soil profile	(–)	1–5000	2532.3	2644.4	(±1505.8)
M	Scaling parameter	(mm)	5–100	37.6	38.8	(±3.8)
T_m	Temperature above which melting occurs	(°C)	–3.88–0.55	–3.17	–3.25	(±0.39)
M_i	Day-degree melting factor	(mm °C ⁻¹ d ⁻¹)	0.46–45.72	9.97	9.84	(±1.17)
V_{rout}	Routing velocity of channel network	(km d ⁻¹)	3–15	13.8	12.50	(±1.54)
N_{eff}	Nash-Sutcliffe efficiency	(–)		0.615	0.606	(±0.006)
Total area		(km ²)	65.63			
Lake area		(km ²)	3.35			
Maximum stream length		(km)	8.3			
Field capacity		(%) ^b	11.36			
Water holding capacity		(%) ^b	16.33			
Soil porosity		(%) ^b	38.79			
Latitude (for ET calculation)		(°) decimal	43.97			
Percent macropore flow		(%)	20			

^aThe best model parameterization based on N_{eff} of the simulated to the observed hydrograph is given as best₁, and best₁₀ represents the 10 best parameter sets given as mean values and standard deviation (SD).

^bGiven as volumetric fractions.

(USGS ID number 04275500), and West Canada Creek near Wilmurt, NY (USGS ID number 01343060) and two gages operated by Myron Mitchell at SUNY College of Environmental Science and Forestry, Archer Creek and Arbutus Lake Outlet. The drainage areas of these catchments included those larger than FB (Hudson = 497 km², Ausable = 1155 km², West Canada = 668 km²) and those smaller than FB (Archer = 1.35 km², Arbutus Outlet = 3.52 km²). To account for differences in timing of catchments of a different size, daily discharge and discharge +1, 2, and 3 days as well as discharge –1, 2, and 3 days was used as variables, which were included if $p < 0.05$. Results of the model were compared to measured flow at FB over the 2007–2008 study period. The correlation was $r^2 = 0.98$, the slope of predicted versus measured flow was 0.98 and the y intercept was $-0.004 \text{ m}^3/\text{s}$ indicating no bias and a slope close to one.

3.2.2. Model Uncertainty and Benchmarking

[30] TOPMODEL uncertainty was derived by applying the ‘Generalized Likelihood Uncertainty Estimation’ (GLUE) [Beven and Binley, 1992] for the simulated hydrograph. This allows a quantification of possible uncertainties originating from parameter choices by applying a variation of model parameters in a reasonable range (Table 1) and analyzing the variation of the output variable. For probability calculations all parameter sets which led to a model result above a given threshold for the objective function ($N_{eff} > 0$) were aggregated. The calculations were performed by the ‘MCAT’ tool developed by Thorsten Wagener (Pennsylvania State University), which is based on the MATLAB platform (The MathWorks, Inc., Natick, MA, USA).

[31] Model Benchmarking was performed by comparing the dynamics of saturated areas simulated with TOPMODEL with a static remotely sensed data set identified and mapped by the Adirondack Park Agency (APA) in which wetlands were delineated according to National Wetland Inventory (NWI) techniques from 1:40000 and 1:58000 scale USGS aerial infrared photos [Canham et al., 2004].

[32] For further comparison a static riparian wetland simulation based on the “vertical distance to stream” method was used for calculating flow directions with a 10 by 10 m DEM by a multiple flow direction algorithm [Seibert and McGlynn,

2007] and determining the stream network as a threshold of accumulated drainage area larger than 2000 cells, which defined a stream area of 1.31% of the total catchment area and which gives the best fit of the delineated stream network compared to the stream represented in the NHD data set. Riparian wetlands were then defined as all areas that have a vertical elevation above the corresponding creek cell (EAC) below a threshold value of 1 m, which spans the range of typical water level fluctuations relative to the river bed in large areas of the FB stream network.

[33] In the TOPMODEL simulations saturation occurs in topographic wetness index classes where the simulated water level reaches the soil surface [Wolock, 1993]. Within this calculation, flat areas were assumed to be always saturated and, thus, they act as static ponds. The number of days in which saturation occurred during the simulation period was counted for each cell for the entire simulation period and spatially mapped. The temporal dynamics of saturation were then compared with the static data sets to calculate a direct spatial coincidence in percent (a cell by cell comparison) represented by k_{match} as shown in equation (3) [Güntner et al., 2004]:

$$k_{match\ a,b} = \frac{n_a}{n_b} \cdot 100[\%] \quad (3)$$

where n_a is the number of spatially coinciding cells in the data sets a and b and n_b is the number of total cells of the data set b in the entire catchment. k_{match} provides therefore the coincidence between the data sets a and b as a percentage of area of data set b .

4. Results

4.1. Temporal Variability of Mercury and DOC Concentrations

[34] During the study period (25 January 2007 to 12 June 2008), total mercury concentrations (THg) in stream water generally showed a more than twofold increase during snowmelt ranging from 1.3 ng L^{-1} to 3.0 ng L^{-1} (Figure 2). The more frequent sampling during the snowmelt 2008

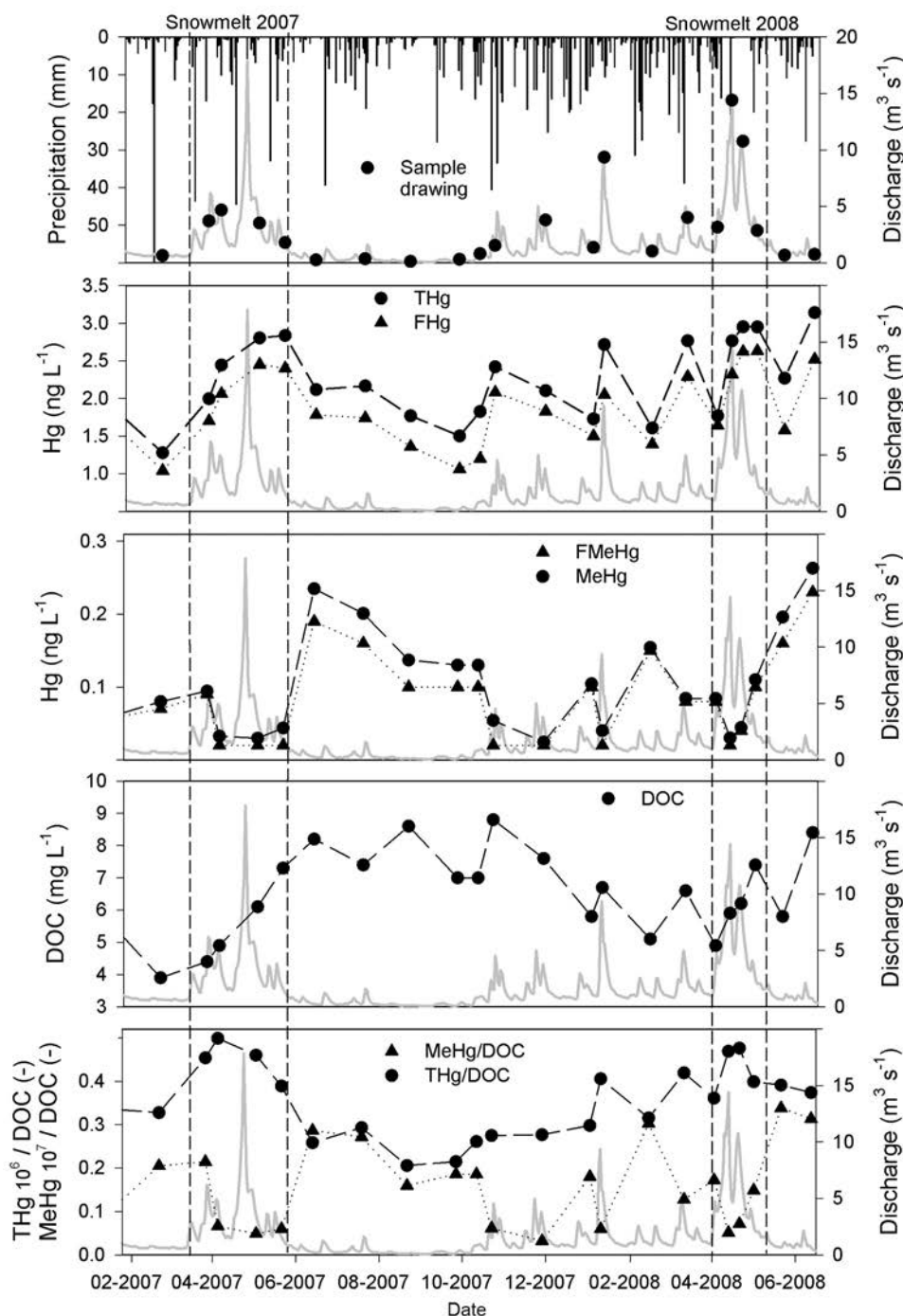


Figure 2. Temporal dynamics of precipitation and discharge (first panel), THg and FTHg (second panel), MeHg and FMeHg (third panel), DOC (fourth panel), and THg:DOC as well as MeHg:DOC ratios (fifth panel) at the outlet of the FB Catchment during the 17 month study period beginning in mid-January 2007. Discharge is presented as a gray line in the background for all panels.

indicated that THg peaked (3.0 ng L^{-1}) during the hydrograph recession. In addition to snowmelt, THg concentrations also showed several peaks at flows that were notably lower than those of snowmelt, and resulted from rainstorms in the fall of 2007 ($2.1\text{--}2.7 \text{ ng L}^{-1}$), and during midwinter thaws (2.8 ng L^{-1}). The highest THg concentration (3.1 ng L^{-1}) was measured during early summer 2008. All THg concentrations were dominated by the dissolved (filtered) fraction with

contributions between 66 and 93% of THg. The highest contributions of particulate Hg (PHg) were observed in October 2007 (34%) and in late May 2008 (30%), whereas PHg concentrations were in the range of $0.13\text{--}0.69 \text{ ng L}^{-1}$, and peaked in May 2008 on the hydrograph recession after the snowmelt 2008. Even though THg concentrations generally increased during events, THg concentrations were not significantly related to discharge. The lack of a strong rela-

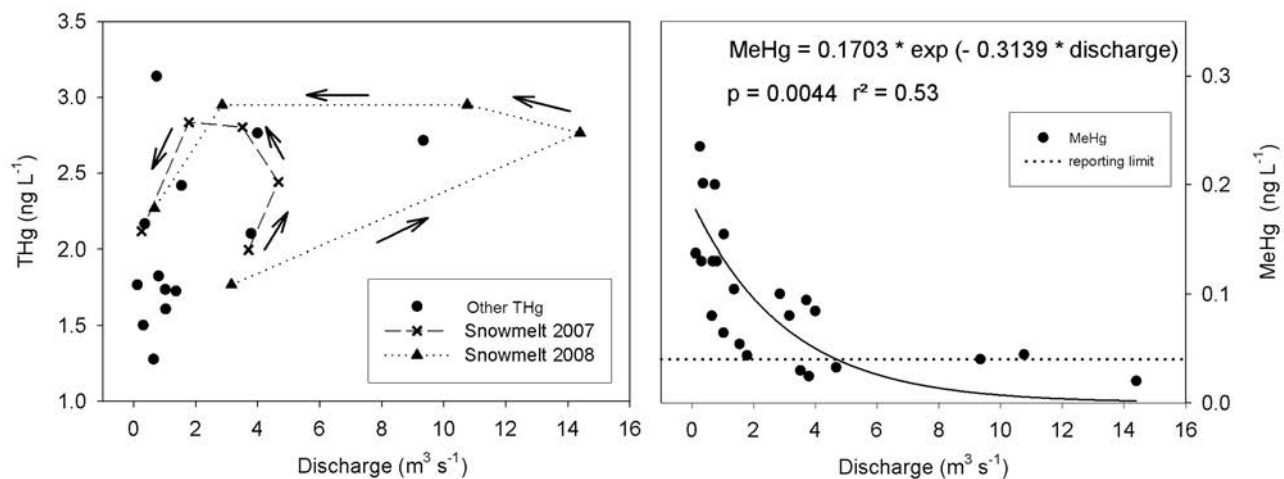


Figure 3. (left) THg versus discharge and (right) MeHg versus discharge for all samples taken during the 17 month study period. During the two snowmelt periods shown in Figure 3 (left), one additional sample before and after each melt period (as specified previously) were added to allow better visualization of the hysteresis effect. Fewer samples were collected during the snowmelt 2007, and as a result, no data point represents concentrations at flows greater than $5 \text{ m}^3 \text{ s}^{-1}$.

tionship can be explained by the uneven Hg flushing behavior with a difference in timing of the discharge peak and the peak in concentration. For both snowmelt periods an uneven flushing with a counterclockwise hysteresis was prevalent (Figure 3).

[35] In contrast total methylmercury concentrations (MeHg) indicate good predictability by a negative log function of discharge ($r^2 = 0.53$, $p = 0.004$; equation given in Figure 3), with values varying between below the detection limit of 0.04 ng L^{-1} and 0.26 ng L^{-1} during the entire study period. The lowest values of MeHg were observed during the two snowmelt periods, and the highest values occurred within 6 weeks after these melt events. The additional measurements during the snowmelt 2008 indicate that the increase of MeHg during and after the snowmelt corresponds with increasing water temperatures (data not shown), decreasing sulfate concentrations (4.7 mg L^{-1} to 3.1 mg L^{-1}), and decreasing dissolved oxygen concentrations (13.4 mg L^{-1} to 8.8 mg L^{-1}), as oxygen saturation decreased from 95% to 88%). Similar to THg, MeHg concentrations reported here were dominated by the dissolved fraction, FMeHg, (37% to 97%), and particulate methylmercury (PMeHg) was the major fraction (>50%) in only two samples collected in May 2007 and early October 2007.

[36] DOC concentrations ranged from 3.9 to 8.8 mg L^{-1} ; the lowest values occurred during winter base flow conditions and the highest value was measured during rewetting after a dry period from August to October 2007. During the winter of 2007–2008, DOC concentrations were between 5.1 mg L^{-1} and 7.6 mg L^{-1} with slightly lower values during the melt period 2008, and the highest concentration (8.4 mg L^{-1}) in June 2008.

[37] The seeps draining shallow wetland groundwater had a median FTHg concentration of 5.3 ng L^{-1} , and the median value was 2.9 ng L^{-1} for the shallow piezometer samples, compared to a median THg value of 2.2 ng L^{-1} for the FB samples. A greater range in FTHg values is evident in the seep and piezometer samples relative to those of THg in FB, and

the highest value in the stream was just slightly greater than the 25% percentile value for the two sets of groundwater values. A Kruskal-Wallis one-way analysis of variance on ranks combined with Dunn's test for all pairwise comparisons indicates that FTHg concentrations in the seeps were significantly greater ($p < 0.025$) than THg concentrations in FB, but that the same difference between piezometer samples and FB samples was not significant. By comparison, the median THg value in the two upland tributaries was 0.9 ng L^{-1} . THg concentrations in these tributaries were significantly less than those of the seeps and piezometers representing runoff generated in riparian wetland areas, but the values were not significantly different than FB as determined by Dunn's method. When just a simple pairwise comparison between the tributaries and FB is performed with a t test (values pass test for normality and equal variance), however, the THg concentrations in the main stem are significantly greater than those of the tributaries.

4.2. Fluxes of THg, MeHg, and DOC

[38] Loads of the three constituents (THg, MeHg and DOC) were strongly dependent on discharge (Table 2). Daily yields of THg as high as $64.0 \text{ ng m}^{-2} \text{ d}^{-1}$ were calculated for the snowmelt 2007. The annual yield was $1.8 \mu\text{g m}^{-2} \text{ yr}^{-1}$ during the 1 year period and the two spring flood periods each accounted for a major fraction of the annual THg load. The 2007 melt load was 57 g, whereas 46% of yearly water yield were discharging. This accounts for 49% percent of the annual THg load of 117 g. The 2008 snowmelt which represents 36% of yearly water yield had a slightly lower THg load (47 g) and accounts for a smaller fraction (40%) of annual THg export. In contrast, MeHg loads during the two melt periods (0.98 g and 1.00 g) were only 25% of the annual MeHg loads during both years, 2007 and 2008. The highest daily yields for MeHg were reached at different times of the year. Values of $60\text{--}720 \text{ pg m}^{-2} \text{ d}^{-1}$ were calculated for snowmelt 2007, $48\text{--}56 \text{ pg m}^{-2} \text{ d}^{-1}$ during the fall of 2007, and

Table 2. Loads and Yields of the FB Catchment^a

	Annual and Snowmelt Yields				Relative Loads				Mean Daily Yields			
	THg ($\mu\text{g m}^{-2}$)	MeHg ^b (ng m^{-2})	DOC (g m^{-2})	Water (mm)	THg (%)	MeHg ^b (%)	DOC (%)	Water (%)	THg ($\text{ng m}^{-2} \text{d}^{-1}$)	MeHg ^b ($\text{pg m}^{-2} \text{d}^{-1}$)	DOC ($\text{mg m}^{-2} \text{d}^{-1}$)	Water (mm d^{-1})
One year	1.8	61.1	4.9	746					4.9	166	13.3	2.0
Melt 2007	0.9	15.3	1.9	345	48	25	39	46	11.4	201	24.8	4.5
Melt 2008	0.7	15.1	1.6	274	40	25	34	37	17.7	368	39.9	6.7

^aThe 1 year period used for the calculations is defined as the time frame from 12 June 2007 to 11 June 2008. The snowmelt periods are 8 March 2007 to 22 May 2007 and 25 March 2008 to 4 May 2008. The column called “relative loads” gives the percentage of the contribution relative to the 1 year period.

^bValues include calculations with FMeHg concentrations below the detection limit (0.04 ng L^{-1}) which were set to 0.02 ng L^{-1} .

further peak yields during the snowmelt 2008 ($64 \text{ pg m}^{-2} \text{ d}^{-1}$). But yields similar to those of the snowmelts were also observed for events with a much smaller hydrological response, such as a small rain event after the snowmelt of 2008, which caused a peak yield of $69 \text{ pg m}^{-2} \text{ d}^{-1}$, whereas stream discharge was just 15% of the 2008 melt peakflow, a result of the greater May–October seasonal response of MeHg concentrations to warmer weather than that of THg concentrations over the study period. We note also that calculations of yields and loads for MeHg during snowmelt have high uncertainty because values of less than the 0.04 ng L^{-1} detection limit were reported in stream water during these periods.

[39] The two melt periods also favored a major export of DOC from the FB catchment. The yield was 1.9 g m^{-2} for the snowmelt 2007 (39% of annual yield), and 1.6 g m^{-2} for snowmelt 2008 (34% of annual yield). Values were also relatively high in the growing season 2007, which accounted for 18% (0.9 g m^{-2}) of the total annual DOC yield, but only 15% of water yield in the stream. The highest calculated daily yields were in the range of 111.8 to $134.1 \text{ mg m}^{-2} \text{ d}^{-1}$, and mainly occurred during the two snowmelt periods as well as during the late summer when major rain events coincided with the highest DOC concentrations. Table 2 gives a summary of all solute exports calculated for this study.

4.3. Relationships Between THg and DOC, Abs₂₅₄

[40] The results indicate a strong, significant relation between THg and DOC in FB upstream of CLF and in the principal tributary to the pond for the six samples collected during the 2007 and 2008 growing seasons, but not downstream at the gage (Figure 4). At the FB stream gage, the coupling of DOC and THg varied by season (Figure 5a). During the nongrowing season, a highly significant ($p < 0.001$) linear relationship ($\text{THg} = -0.304 + 0.454 (\text{DOC})$) which explains a large part of the variation ($r^2 = 0.63$) was found, whereas no significant relationship could be established for the growing season. A similar pattern was found for the relation of Abs₂₅₄ and THg concentrations (Figure 5b). A highly significant linear relationship for the nongrowing season ($\text{THg} = 0.030 + 10.414 (\text{Abs}_{254})$) showed similar explanatory power to that of the DOC relationship ($r^2 = 0.63$; $p < 0.001$), whereas a weaker, but still significant relationship was found for the growing season ($\text{THg} = -0.407 + 8.792 (\text{Abs}_{254})$; $r^2 = 0.46$, $p = 0.038$).

4.4. Modeling Results

4.4.1. Hydrological Response and Model Benchmarking

[41] The hydrograph simulated with the rainfall/runoff model TOPMODEL is in broad agreement with the discharge

measured at the outlet of the FB catchment. The best model fit generally represents the strongly snowmelt influenced hydrograph resulting in a matching between simulated and measured flow of $N_{\text{eff}} = 0.615$ with a root mean square error (RMSE) of 0.23. The best parameter set (best₁) as well as the means and standard deviations (SD) of model parameterizations representing the 10 best model runs (best₁₀) as determined by N_{eff} are given in Table 1.

[42] The first simulated snowmelt period (winter 2005/06) was used as a warm up period, and these results are excluded from the calculations of model performance described here. During the 2006–2008 study period, the winter season shows the best simulations. The hydrograph of the accumulation period 2006/2007 (not shown) and a short melt in early January 2007 (Figure 6) are well reproduced. The following melt period in April 2007 (snowmelt 2007) is simulated well, though a small false discharge peak was simulated early in the melt. In the following phase of summer low flow, the model represents the measured hydrograph, but overestimates the response of the catchment to rain events (Figure 6). The simulations for the winter 2007/2008 are also close to the observed discharge patterns in the stream. During the snow accumulation period (winter 2007–2008) some rain events

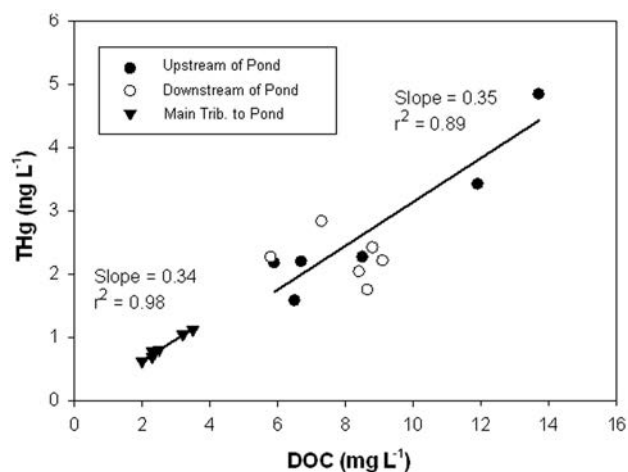


Figure 4. THg and DOC concentrations in the Fishing Brook catchment for six samples collected during the growing season of 2007 and 2008 at each of three sampling sites located upstream of the pond, at the downstream end of the pond (at gage; County Line Flow), and at the principal tributary entering the pond. A statistically significant relation ($p < 0.05$) between THg and DOC was observed upstream of the pond and in the tributary, but no relation was evident at the downstream end of the pond on the sampling dates.

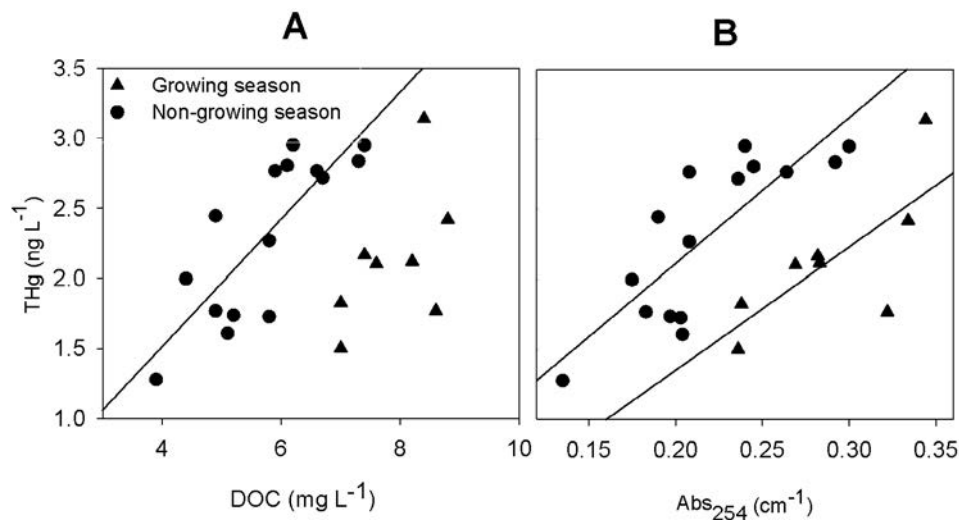


Figure 5. (a) THg versus DOC and (b) THg versus Abs_{254} for all samples taken during the 17 month study period. The drawn lines represent linear relationships which were found as $THg = -0.304 + 0.454 (DOC)$ for THg versus DOC (Figure 5a) during the nongrowing season ($r^2 = 0.63$; $p < 0.001$). The equations for THg versus Abs_{254} (Figure 5b) are given as $THg = 0.030 + 10.414 (Abs_{254})$ with $r^2 = 0.63$; $p < 0.001$ for the nongrowing season and $THg = -0.407 + 8.792 (Abs_{254})$ with $r^2 = 0.46$; $p = 0.038$ for the growing season.

led to small responses of stream flow, which were not simulated by the simple snowmelt routine. However, the snowmelt 2008 is well reproduced with flow volumes and the timing of both peaks corresponding closely with the measured flow.

[43] Even though the “best fit” model did not show good agreement for some periods, only in a few time periods of short duration did the measured hydrograph not fall within the range given by the GLUE confidence limits (Figure 6). These periods not covered within the GLUE uncertainty ranges were (1) the snow accumulation period during January and February 2007, when the measured flow was lower than the lowest model realizations which were not rejected (Figure 6), and (2) a short period before the major melt event of 2007 and after the melt of 2008, during which the model bounds predict higher flows.

[44] The extent of simulated saturated areas (A_{sat}) varied between 6% and 12% of the total catchment area during the 17 month study period (Figure 6). This includes 5% of the catchment assumed to be constantly saturated (cells with open water plus adjacent cells with the same elevation as open water or stream cells) and was referred to as lake area within the model (Table 1). The average soil storage deficit D_s shows a similar, but inverse relationship with A_{sat} . The highest extent of A_{sat} was calculated for the period with the lowest storage deficits, the snowmelts of 2007 and 2008, whereas the lowest extent of saturated area was predicted for the summer (Figure 6). However, we note that when TOPMODEL is applied in a semidistributed manner as here with lumped parameters for soil properties such as infiltration capacity and soil depth, A_{sat} shows an inverse exponential relationship with D_s , as can easily be seen from formulations given by *Beven* [1997].

4.4.2. Modeled Saturated Area and Static Wetland Estimates

[45] Total wetland area was calculated as 7.0 km² for the APA data set, 9.1 km² for the EAC approach and

TOPMODEL saturation varied between 3.4 km² and 12.3 km². When comparing the spatial agreement of wetlands mapped by the APA as well as the EAC riparian wetland simulations to A_{sat} on a cell by cell basis the spatial congruence between the data sets varies with the frequency distribution of saturated area extent simulated with TOPMODEL. In Table 3 the congruence of the data sets is described according to the relative frequencies of exceedance, which expresses the number of days during which the cell was simulated to be saturated by TOPMODEL and was also a wetland according to the nondynamic data sets divided by the number of days of the entire simulation period. The congruence expressed as $k_{match\ TOP, APA}$ ranges from 38% to 64%, whereas the APA data set specifies 11% of the catchment as wetlands. The lowest overlap (38%) of the two data sets is calculated to be exceeded for the entire simulation period (896 days); however, for high-flow events such as the snowmelt events, the spatial congruence increases to 64% for a frequency of just 1.1×10^{-3} , which represents a duration of just 1 day. Additionally, EAC includes 14% of the catchment area, and a $k_{match\ TOP, EAC}$ of 31% was calculated for the entire simulation period, whereas a peak of 69% of the calculated riparian area was congruent with the TOPMODEL saturated area for 1 day of high flow during peak snowmelt 2008. The spatial congruence between the two static data sets (APA and EAC) resulted in a $k_{match\ EAC, APA}$ of 67%. Some differences in these calculations are not surprising given the heterogeneity of the landscape and that most, but not all wetlands occur in areas with high *TWI*, such as stream corridors. Some of the variable source areas are therefore expected to lie outside of stream riparian areas. In summary, the congruence between saturated cells in TOPMODEL and both APA wetland cells and EAC riparian cells is greatest for the days when the catchment is wettest, but this congruence was never more than 70% of the cells. These calculations provide support that TOPMODEL-derived saturated area calculations serve as a good surrogate for the tendency of solute flushing into the streams due

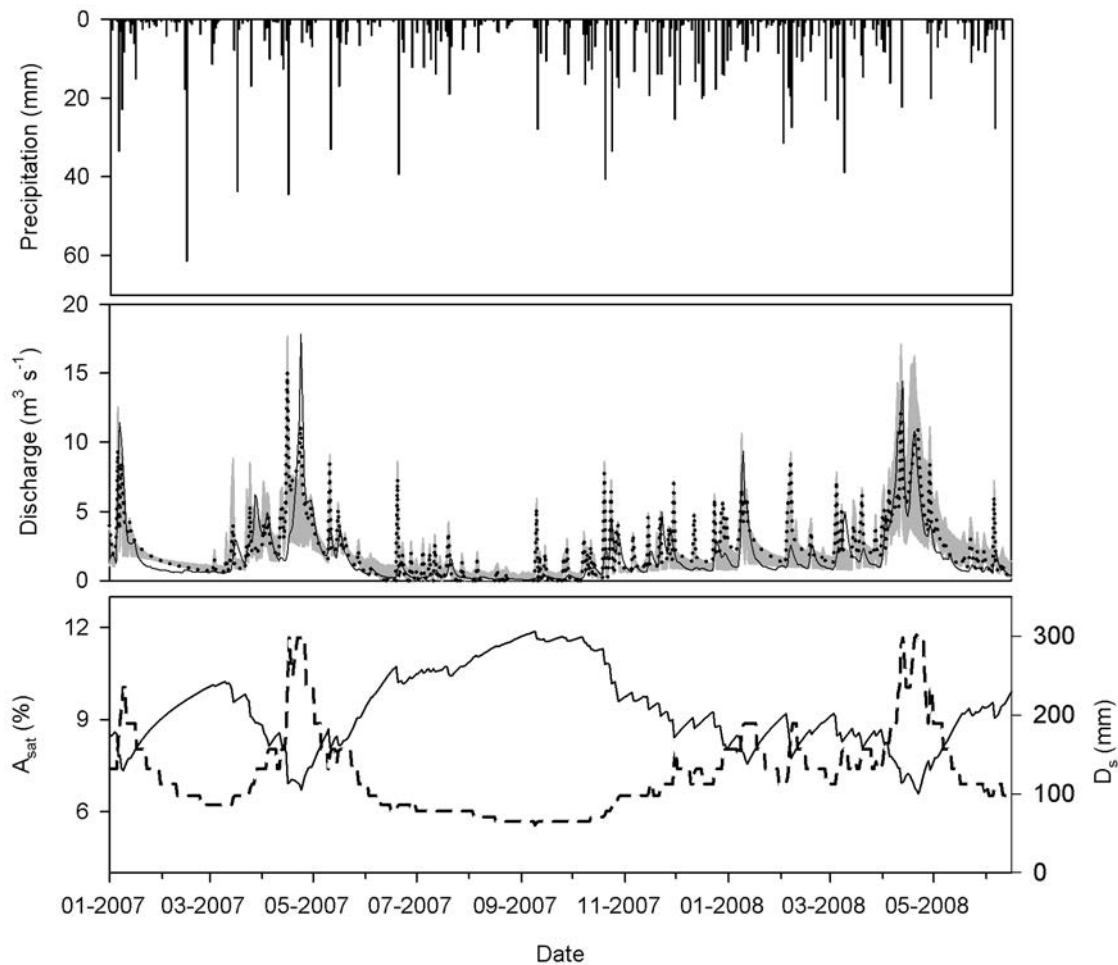


Figure 6. TOPMODEL results for the study period from January 2007 to June 2008. Shown is (top) daily precipitation, (middle) measured and simulated discharge (solid and dotted line, respectively), as well as the simulated uncertainty intervals for discharge simulated with GLUE derived from all model runs performing with a Nash-Sutcliffe efficiency (N_{eff}) above 0.0 (gray shading). (bottom) The dynamics of simulated saturated area (A_{sat} ; dashed line) as well as soil storage deficit (D_s ; solid line) derived from the best fit model parameterization as determined by N_{eff} .

Table 3. Spatially Distributed Cell-by-Cell Comparison of the TOPMODEL Dynamic of Simulated Saturated Areas (TOP) With Static Wetland Mapping Determined by Remote Sensing (APA) and Static Riparian Buffer Wetland Simulations Based on the Vertical Distance of Slope Cells to Stream Cells Method (EAC)^a

Frequency of Exceedance	TOP Simulated Saturation, A_{sat} (%)	APA Remote Sensing, $k_{match\ TOP, APA}$ (%)	EAC Riparian Buffer, $k_{match\ TOP, EAC}$ (%)
0.001	18.62	63.6	68.8
0.011	14.98	57.8	62.1
0.015	12.39	53.0	56.4
0.023	10.56	49.7	52.0
0.052	9.25	47.3	48.7
0.118	8.31	45.5	46.1
0.232	7.62	44.1	43.8
0.407	7.08	43.0	41.9
0.583	6.67	42.2	40.1
0.723	6.36	41.6	38.6
0.848	6.12	41.1	37.3
0.934	5.92	40.6	36.2
0.997	5.76	40.1	35.2
1.000	5.20	38.2	31.4
$k_{match\ EAC, APA}$			66.8%

^aThe columns marked k_{match} indicate the extent to which the TOP saturation coincides with the total number of APA wetland and EAC riparian cells, respectively, for each level of exceedance frequency, as defined in equation (3) in the text.

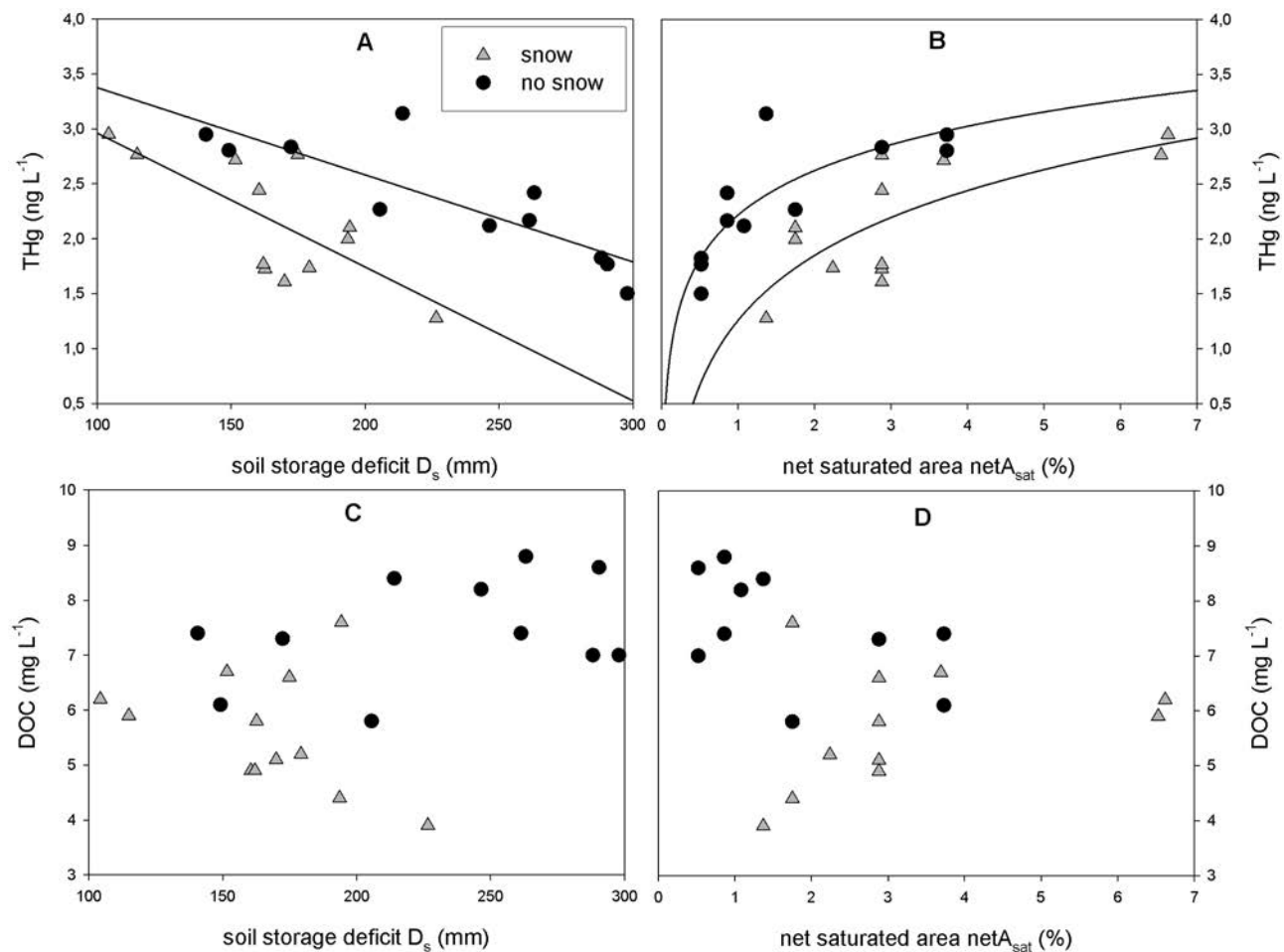


Figure 7. (a and c) Mercury (THg) and DOC concentrations in FB as a function of simulated soil storage deficit and (b and d) the simulated additional saturated area during the 17 month study period for each of snow and no snow periods. The indication of snow/no snow periods is based on the presence of snow simulated by the TOPMODEL snowmelt routine. Drawn lines represent relationships which are given as $\text{THg} = 4.169 - 0.008 (D_s)$; $r^2 = 0.53$; $p < 0.001$ for the snow season and $\text{THg} = 4.179 - 0.012 (D_s)$; $r^2 = 0.72$; $p < 0.001$ for the nonsnow season (difference $p < 0.05$) for Figure 7a. Nonlinear relationships (Figure 7b) are given as $\text{THg} = 1.259 \cdot 0.854 \ln(\text{netA}_{\text{sat}})$ with $r^2 = 0.50$; $p < 0.001$ for the snow season and $\text{THg} = 2.218 \cdot 0.582 \ln(\text{netA}_{\text{sat}})$ with $r^2 = 0.66$; $p < 0.001$ for the nonsnow season. No significant relationships were found for DOC versus D_s as well as DOC versus netA_{sat} .

to a wetting-up of the catchment and, consistent with our hypothesis, this process should be the most important for mobilization of Hg into the stream network.

4.4.3. Relationships Between Simulated Saturation State and Solute Concentrations

[46] The comparison of the two lumped variables used within TOPMODEL simulations to describe the catchment saturation state, D_s and A_{sat} with measured THg and DOC concentrations shows a seasonally varying behavior, dependent on the availability of snow simulated with TOPMODEL (Figure 7). For the winter season (simulated presence of a snowpack according to TOPMODEL), a strong linear relationship between D_s and THg was evident ($\text{THg} = 4.169 - 0.008 (D_s)$; $r^2 = 0.53$; $p < 0.001$), whereas the relationship during summer ($\text{THg} = 4.179 - 0.012 (D_s)$; $r^2 = 0.72$; $p < 0.001$) was even stronger. A similar pattern was observed when comparing THg to the net simulated saturated area

(netA_{sat}), defined as the saturation in addition to the always saturated 5% of the catchment (Figure 7b) given in percent of the total area. During the winter season, a logfunction ($\text{THg} = 1.259 \cdot 0.854 \ln(\text{netA}_{\text{sat}})$) explained slightly more than half of the variation ($r^2 = 0.50$; $p < 0.001$). For the summer season, the log function $\text{THg} = 2.218 \cdot 0.582 \ln(\text{netA}_{\text{sat}})$ was a better predictor ($r^2 = 0.66$) with a similar significance level ($p < 0.001$).

[47] No significant relationships were found between DOC and D_s , even though the data set seems to indicate opposing behavior in the winter and summer seasons. During times with a simulated snowpack stream DOC concentrations seem to increase as storage deficit decreases, whereas during summer DOC concentrations seem to increase with increasing D_s (Figure 7c). When comparing netA_{sat} to DOC concentrations (Figure 7d) the same pattern seems to be

confirmed, but no significant relationships could be identified here either.

5. Discussion

5.1. Solute Concentrations

[48] The ranges of stream Hg concentrations measured in this study correspond well with those of other studies in the northeastern United States. The mean THg concentration at FB over the 17 month study period was $2.2 \pm 0.5 \text{ ng L}^{-1}$. At the nearby Archer Creek watershed, which is a downstream tributary to FB, values of $1.8 \pm 1.3 \text{ ng L}^{-1}$ have been reported for upland areas, and $3.2 \pm 2.3 \text{ ng L}^{-1}$ downstream of wetland areas over a 2 year period (2004–2006) [Selvendiran *et al.*, 2008]. Sharp increases in THg concentrations were also reported at this site during summer storms sampled in 2005 with values that ranged from 1.1 to 5.7 ng L^{-1} in upland areas and 2.8 to 7.4 ng L^{-1} downstream of the wetlands [Bushey *et al.*, 2008]. This work highlights the role of well connected riparian wetlands on increasing THg concentrations, similar to results in many other forested northern watersheds [Galloway and Branfireun, 2004; Mitchell *et al.*, 2008c]. One difference from Archer Creek is that the river network in the larger FB catchment includes more ponds and a greater proportion of wetland areas that store water and may diminish variation in THg concentrations, as reflected by the lower standard deviation of these values at FB than at Archer Creek.

[49] The MeHg concentrations observed in FB ($0.10 \pm 0.07 \text{ ng L}^{-1}$) also correspond well with studies at Archer Creek where values of 0.04 ± 0.03 and $0.17 \pm 0.15 \text{ ng L}^{-1}$ were measured in the upland stream and downstream of wetland areas, respectively [Selvendiran *et al.*, 2008]. Other studies of northern U.S. watersheds influenced by riparian wetlands such as those at the Marcel Experimental Forest in Minnesota show similar to slightly higher ranges of MeHg values of 0.12 ± 0.05 and $0.28 \pm 0.10 \text{ ng L}^{-1}$ for watershed S2 and S6, respectively [Mitchell *et al.*, 2008c]. When comparing FB and Archer Creek, variation in MeHg concentrations as represented by the SD is higher in Archer Creek downstream of the wetland, but not upstream. Observed DOC concentrations follow the same pattern. The values at FB ($6.5 \pm 1.4 \text{ mg L}^{-1}$) are bounded by the values in Archer Creek upstream ($3.5 \pm 1.6 \text{ mg L}^{-1}$) and downstream ($7.6 \pm 6.1 \text{ mg L}^{-1}$) of the riparian wetland. Even though THg and DOC concentrations are in a similar range for both of these study sites in the Adirondack Mountains, some clear differences are evident as well. Strong relationships between THg and DOC concentrations have been observed at Archer Creek as well as at a number of other forested watersheds in the northeastern United States (Hubbard Brook Experimental Forest (HBEF), NH; Sleepers River Watershed (SRW), VT; Lake Champlain headwaters, VT). These data collected across varying hydrologic conditions and seasons, show correlation coefficients between THg and DOC concentrations that range from 0.78 to 0.92 and even stronger relationships between THg concentrations and Abs_{254} , ($r^2 = 0.89$ to 0.94) [Dittman *et al.*, 2009]. These same strong relationships were not evident at the FB Catchment. Here, the correlations are strongly seasonal (Figure 5), suggesting that seasonally variable processes may affect DOC and THg sources and transport at FB that are not evident at many other nearby catchments.

5.2. Runoff Generation and Hg Flushing Mechanisms

[50] The fairly high congruence of up to 64% between the simulated saturated areas by TOPMODEL and the APA remotely sensed wetlands when the catchment is at a high-saturation state, indicates that most of the areas likely to be saturated at high-flow conditions are located in wetlands, which are dominantly in riparian areas in this catchment. Therefore, we conclude that our simulations provide a robust estimation of runoff generation even if the observed N_{eff} values of the 10 best model runs (0.606 ± 0.006) for the streamflow are low when compared to those of other studies [e.g., Ambroise *et al.*, 1996]. The higher congruence of up to 69% between the EAC riparian wetland simulation and modeled saturation at high flow further suggests that a large proportion of these wetlands are well connected to the stream network. Furthermore, if water levels in these areas rise and near-surface flow pathways are activated, the simulation indicates that saturation overland flow can occur in these wetland areas, in valley bottoms, and in gently sloping areas at the transition from hillslopes to wetlands. Finally, if these areas act as source areas for THg, the relationships of THg to netA_{sat} suggest that these high-flow conditions with a high-saturation state cause near-surface runoff generation that in turn result in a high rate of Hg flushing during snowmelt.

[51] Recent studies focusing on the W6 watershed at HBEF [Demers *et al.*, 2010] and three different forested watersheds (W6 at HBEF; SRW; Archer Creek) [Dittman *et al.*, 2010] indicate that for smaller upland areas, the flushing of THg and DOC is strongly controlled by changing source areas with linear or exponential increases in THg concentrations with discharge [Demers *et al.*, 2010; Dittman *et al.*, 2010].

[52] The results of the current study (Figure 8), differ from those discussed above because the study catchments differ in at least three aspects: (1) FB is a much larger catchment than those studied at HBEF, SRW, and Archer Creek, (2) FB has distinctly different geographic source areas for runoff in the extensive riparian area dominated by wetlands and in the upland tributaries that are more similar to these other catchments (Archer Creek has some wetland area), and (3) FB has open water bodies. These differences in drainage area, geomorphology, and in the extensiveness of wetlands results in differences in runoff sources of Hg to the stream compared to HBEF, SRW, and Archer Creek. Runoff from shallow groundwater sources in the riparian area is likely the principal source of Hg during snowmelt, and seeps and shallow piezometers in the largest riparian wetland area in the FB catchment generally have higher FTHg concentrations than those (THg) in FB at the County Line Flow gage, whereas upland tributaries have lower THg concentrations, that are insufficient to cause the flushing patterns of Hg observed in this study. The wetland area where groundwater was collected is also primed to contribute runoff because of a shallow water table; for example at 14 of the 15 shallow piezometers for which FTHg values were presented in Figure 8, median water table depth on May 5 and 6, 2009 was 232 mm below land surface, during a period when the discharge at FB was very close ($1.9 \text{ m}^3/\text{s}$) to the mean value for the Jan. 2007 through June 2008 study period ($1.7 \text{ m}^3/\text{s}$) considered in this paper, and the water table is likely to have been at even shallower depths in the spring at the time of snowmelt. These data are consistent with the description of these soils as being

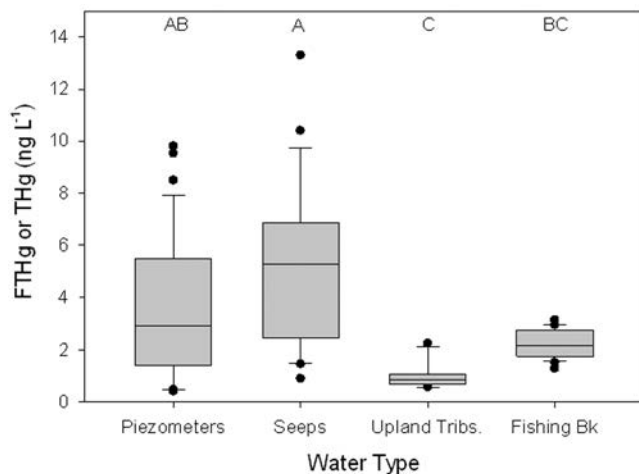


Figure 8. Hg concentrations in: (1) piezometers and (2) seeps located in the Six Mile Brook riparian wetland, (3) in two upland tributaries to Fishing Brook with no wetlands and little riparian area, and (4) in Fishing Brook. Values are FTHg for piezometers and seeps and THg for upland tributaries and Fishing Brook. A Kruskal-Wallis one-way analysis of variance on ranks was performed, and results indicated the median values of the four groups were statistically different. The letter designation then indicates the results of all pairwise comparisons using Dunn's method. Those with similar letters are not significantly different, and a difference in the letters indicates a significant difference.

“poorly to very poorly drained” (but with moderately high to high saturated hydraulic conductivity), and with TOPMODEL results that indicate that such riparian wetland areas are where surface saturation and flushing of Hg occurs during snowmelt and other high-flow periods. In contrast, the tributaries that drain steep upland parts of the catchment with little or no measured wetland area, and narrow riparian areas indicate little opportunity for expansive surface saturation. This upland landscape represents 89% of the catchment area of FB, and runoff from this part of the catchment would tend to dilute THg concentrations in FB (DOC is similarly much lower in these upland tributaries than in FB, data not shown), and therefore this part of the landscape is not likely a major source of the flushing effect of increasing THg concentrations observed in FB. Together, these data support the conceptualization that riparian areas where wetlands are predominant are the major source areas for the flushing of Hg into FB that was observed and simulated with TOPMODEL in this study.

[53] The flushing of MeHg is in contrast less strongly controlled by saturated areas and follows an inverse log relationship to discharge (Figure 3). MeHg concentrations decrease with increasing discharge, a pattern that has been observed in other catchments, particularly those dominated by snowmelt in cold winter climate locations [Bishop *et al.*, 1995; Branfireun and Roulet, 2002; Mitchell *et al.*, 2008c]. The observed pattern with discharge was no doubt greatly influenced by the collection of most high-flow samples during snowmelt; catchments often show increasing MeHg concentrations with discharge during storms in the growing season [Shanley *et al.*, 2008]. This inverse logarithmic relationship indicates that for high runoff, the supply of mobile

MeHg from areas of high methylation rates is limited relative to hydrologic flux rates. Such a limitation of available MeHg for flushing during high flow is also suggested by Demers *et al.* [2010] for the W6 upland watershed of the HBEF. For this watershed, however, discharge could explain little of the [MeHg] variation, which in contrast to FB peaked early on rising limb of the hydrograph. This difference of FB compared to W6 at HBEF could be explained by the rapid production of MeHg during the snowmelt recession (Figure 2 and Figure S8) in FB which may compensate for the MeHg loss in the soils during the snowmelt flushing events. This type of supply limited flushing behavior suggests that the export of MeHg is more strongly dependent on factors that control the direct production of MeHg such as soil temperatures [Ramlal *et al.*, 1993; Ullrich *et al.*, 2001], and the availability of sulfate and labile organic carbon [Mitchell *et al.*, 2008a] than on hydrologically favorable flushing conditions.

[54] The weak relationship between THg and DOC concentrations in FB during the summer season suggests greater independence of either the hydrologic or biogeochemical processes that affect DOC and THg transport at this time of year and suggests at least two possibilities. First, DOC and THg sources in the warm season may differ from the dominant sources during the cold season, which might cause different responses of DOC and THg and therefore no strong relationship between these two solutes. This source could be within the stream corridor, such as DOC derived from decaying algae, aquatic plants, and stream bank/bottom sediment. DOC that is derived from in-stream sources generally is more aliphatic, with lesser ability to complex metals such as Hg than the more aromatic DOC derived from catchment soils [Weishaar *et al.*, 2003; Dittman *et al.*, 2009]. Alternatively, a greater proportion of DOC could be derived from wetland soils than upland soils during the warm season, and delivered disproportionately (relative to Hg) to the stream via groundwater transport from riparian wetland areas. Lower Hg:DOC in wetlands than in uplands has been observed in other studies [Mitchell *et al.*, 2008c]. This seasonal shift in hydrology is likely part of the normal seasonal progression in catchments with large riparian wetland area where summer drying of the catchment results in less flow originating from upland areas. This seasonal hydrologic disconnection has been observed in other temperate catchments [Devito *et al.*, 1996; Hill, 2000]. The result in either case would be less THg mass per unit of DOC mass, consistent with the observations shown in Figure 4. Interestingly, recent work in Swedish boreal catchments indicates that DOC derived from wetlands tends to have greater specific Abs₂₅₄ values per mg of DOC (SUVA₂₅₄) indicating greater aromaticity of DOC in wetlands than in surrounding forested uplands [Ågren *et al.*, 2008]. If this pattern were prevalent at FB and the sources of DOC would shift from greater upland contribution to greater wetland contribution during summer, we would expect a shift in SUVA₂₅₄ to higher values during the growing season. Further we would expect higher concentrations of THg per mg of DOC because of the strong link between aromaticity as estimated by Abs₂₅₄ and THg concentrations in surface waters [Dittman *et al.*, 2009]. Instead, we find the opposite behavior in our data set; SUVA₂₅₄ shifts from average values (\pm SD) of $3.6 (\pm 0.25) \times 10^{-2}$ during the growing season to $3.8 (\pm 0.21) \times 10^{-2}$ during the nongrowing

season with less THg per mg of DOC in summer than in winter.

[55] The changing THg – DOC patterns from winter to summer could also be related to in-stream losses of THg that are not paralleled by comparable in-stream losses of DOC. The small pond, County Line Flow immediately upstream of the gage in FB strongly modifies the THg-DOC relationship (Figure 4). This pattern cannot be explained by simple mixing, which would result in values that should lie along the line defined by upstream and tributary samples, since the two significant relations have nearly identical slopes (Figure 4). Instead these data indicate that the net effect of biogeochemical processes within CLF is to alter the relation between THg and DOC. We cannot with certainty identify the processes responsible for altering the THg-DOC relation, but several processes known to occur in ponded settings are possible.

[56] County Line Flow is a shallow pond with a mean depth of 0.5 m and despite a mean residence time of 1 day, this time increases during low-flow conditions in the growing season, and averaged 3 days during the six sampling periods. Such conditions (long days, shallow depth, and a multiday residence time) would favor alteration of both Hg and DOC by photolytic processes such as reduction of Hg(II) to Hg⁰ and enhanced degradation of DOC, which have been demonstrated in both field and laboratory experiments [Wetzel et al., 1995; Peters et al., 2007]. Other processes involving interaction with bottom sediments, and alteration of the aromaticity of DOC and resulting effects on the ability of DOC to bind with and transport Hg are possible as well. The relations of THg to Abs₂₅₄ (data not shown) in the pond are very similar to those observed with DOC, strong significant relations of THg and Abs₂₅₄ in FB upstream of the pond and in the principal tributary, but no relation at the downstream end of the pond suggesting that a large change in the character of DOC to favor greater ability to bind with Hg did not occur in this impoundment. The SUVA₂₅₄ was slightly lower (mean = 3.8, SD = 0.2 × 10⁻²) downstream of the pond than upstream (mean = 4.0, SD = 0.2 × 10⁻²) on the six sampling dates, which is consistent with a slight increase in the aliphatic character of the DOC due to an algal source, but this difference is not great, and likely does not completely explain the shift in the THg-DOC relation through CLF. Nonetheless, the data shown in Figure 4 do provide evidence that transport through impoundments in the FB catchment alters and weakens the THg-DOC relationship.

6. Conclusions

[57] Similar to other studies [Bishop et al., 1995; Mitchell et al., 2008c; Schuster et al., 2008; Demers et al., 2010] this study indicates that snowmelt is a major period for Hg transport during the year, and accounts for a relatively large proportion of annual export that ranged from 40% to 48% during 2007 and 2008 in FB. Even though the snowmelt export of DOC compared to the yearly load was also high (34–39%), the results presented here show a weaker relation between DOC and THg concentrations than reported previously for surface waters of the Adirondack Mountains [Driscoll et al., 1995; Dittman et al., 2009], suggesting that different and seasonally varying processes affect the net mobilization of these two constituents. The large drainage area and heterogeneous landscape with streams and ponds

that characterizes FB relative to many of the other catchments in the Adirondacks and elsewhere that show strong DOC-THg relations, may explain the differing mobilization behavior observed in the current study.

[58] The model application strongly suggests that the connection of riparian wetlands and wetland/upland transition zones is the major control of THg net mobilization to surface waters on an annual basis. Further the modeling approach suggests that the mobilization behavior of DOC differs from that of THg in the FB catchment. The most likely reasons for this differing behavior are: (1) a seasonal shift of dominant sources of flow and organic carbon from uplands plus riparian wetlands during wet conditions such as snowmelt to just wetlands during dry conditions that typically occur in summer, and (2) in-stream/pond processes that have differing and divergent effects on Hg and DOC mobilization. Deciphering the relative role of these processes will require additional process-focused research and highlights the need for additional studies in heterogeneous basins in the range of 10s of km² or larger.

[59] **Acknowledgments.** Funding for the research was provided by the U.S. Geological Survey National Water Quality Assessment Program (NAWQA). A particular thanks to John Byrnes (USGS) for excellent support in the field and Christoph Külls for additional lab analysis at the University of Freiburg, Germany. Additional logistical support was provided by the Adirondack Ecological Center operated by SUNY-ESF. Further we thank Jamie Shanley, Mark Brigham, and David Wolock for useful comments on an earlier version of this manuscript.

References

- Ågren, A., I. Buffam, M. Berggren, K. Bishop, M. Jansson, and L. Laudon (2008), Dissolved organic carbon characteristics in boreal streams in a forest-wetland gradient during the transition between winter and summer, *J. Geophys. Res.*, *113*, G03031, doi:10.1029/2007JG000674.
- Ambroise, B., J. Freer, and K. Beven (1996), Application of a generalized TOPMODEL to the small Ringelbach catchment, Vosges, France, *Water Resour. Res.*, *32*(7), 2147–2159.
- Benoit, J. M., C. C. Gilmour, A. Heyes, R. P. Mason, and C. L. Miller (2003), Geochemical and biological controls over methylmercury production and degradation in aquatic ecosystems, in *Biogeochemistry of Environmentally Important Trace Elements*, edited by Y. Cai and O. C. Braids, pp. 262–297, Am. Chem. Soc., Washington, D. C.
- Beven, K. (1997), TOPMODEL: A critique, *Hydrol. Process.*, *11*(9), 1069–1085.
- Beven, K., and A. Binley (1992), The future of distributed models: Model calibration and uncertainty prediction, *Hydrol. Process.*, *6*(3), 279–298.
- Beven, K. J., and M. J. Kirkby (1979), A physically based, variable contributing area model of basin hydrology, *Hydrol. Sci. Bull.*, *24*(1, 3).
- Bishop, K., Y. H. Lee, C. Pettersson, and B. Allard (1995), Methylmercury in runoff from the Svartberget catchment in northern Sweden during a stormflow episode, *Water Air Soil Pollut.*, *80*(1–4), 221–224.
- Boyer, E. W., G. M. Hornberger, K. E. Bencala, and D. M. Mcknight (1997), Response characteristics of DOC flushing in an alpine catchment, *Hydrol. Process.*, *11*(12), 1635–1647.
- Branfireun, B. A., and N. T. Roulet (2002), Controls on the fate and transport of methylmercury in a boreal headwater catchment, northwestern Ontario, Canada, *Hydrol. Earth Syst. Sci.*, *6*(4), 785–794.
- Brigham, M. E., D. A. Wentz, G. R. Aiken, and D. P. Krabbenhoft (2009), Mercury cycling in stream ecosystems. 1. Water column chemistry and transport, *Environ. Sci. Technol.*, *43*(8), 2720–2725.
- Brown, V. A., J. J. McDonnell, D. A. Burns, and C. Kendall (1999), The role of event water, a rapid shallow flow component, and catchment size in summer stormflow, *J. Hydrol.*, *217*(3–4), 171–190.
- Burns, D. A. (2005), What do hydrologists mean when they use the term flushing?, *Hydrol. Process.*, *19*(6), 1325–1327.
- Burns, D. A., P. S. Murdoch, G. B. Lawrence, and R. L. Michel (1998), Effect of groundwater springs on NO₃⁻ concentrations during summer in Catskill Mountain streams, *Water Resour. Res.*, *34*(8), 1987–1996.
- Bushey, J. T., C. T. Driscoll, M. J. Mitchell, P. Selvendiran, and M. R. Montesdeoca (2008), Mercury transport in response to storm events from a northern forest landscape, *Hydrol. Process.*, *22*(25), 4813–4826.

- Butler, T. J., M. D. Cohen, F. M. Vermeulen, G. E. Likens, D. Schmeltz, and R. S. Artz (2008), Regional precipitation mercury trends in the eastern USA, 1998–2005: Declines in the Northeast and Midwest, no trend in the Southeast, *Atmos. Environ.*, *42*(7), 1582–1592.
- Canham, C. D., M. L. Pace, M. J. Papaik, A. G. B. Primack, K. M. Roy, R. J. Maranger, R. P. Curran, and D. M. Spada (2004), A spatially explicit watershed-scale analysis of dissolved organic carbon in Adirondack lakes, *Ecol. Appl.*, *14*(3), 839–854.
- Choi, H. D., and T. M. Holsen (2009), Gaseous mercury fluxes from the forest floor of the Adirondacks, *Environ. Pollut.*, *157*(2), 592–600.
- Choi, H. D., T. J. Sharac, and T. M. Holsen (2008), Mercury deposition in the Adirondacks: A comparison between precipitation and throughfall, *Atmos. Environ.*, *42*(8), 1818–1827.
- Christophersen, N., and R. P. Hooper (1992), Multivariate analysis of stream water chemical data: The use of principal components analysis for the end-member mixing problem, *Water Resour. Res.*, *28*(1), 99–107.
- Demers, J. D., C. T. Driscoll, and J. B. Shanley (2010), Mercury mobilization and episodic stream acidification during snowmelt: Role of hydrologic flow paths, source areas, and supply of dissolved organic carbon, *Water Resour. Res.*, *46*, W01511, doi:10.1029/2008WR007021.
- Devito, K. J., A. R. Hill, and N. Roulet (1996), Groundwater-surface water interactions in headwater forested wetlands of the Canadian Shield, *J. Hydrol.*, *181*(1–4), 127–147.
- DeWild, J. F., M. L. Olson, and S. D. Olund (2002), Determination of methyl mercury by aqueous phase ethylation, followed by gas chromatographic separation with cold vapor atomic fluorescence detection, 14 pp., *U.S. Geol. Surv. Open File Rep.*, 01–445.
- DeWild, J. F., S. D. Olund, M. L. Olson, and M. T. Tate (2004), Methods for the preparation and analysis of solids and suspended solids for methylmercury, 21 pp., *U.S. Geol. Surv. Tech. Methods Rep.*, 5–A7.
- Dittman, J. A., J. B. Shanley, C. T. Driscoll, G. R. Aiken, A. T. Chalmers, and J. E. Towse (2009), Ultraviolet absorbance as a proxy for total dissolved mercury in streams, *Environ. Pollut.*, *157*(6), 1953–1956.
- Dittman, J. A., J. B. Shanley, C. T. Driscoll, G. R. Aiken, A. T. Chalmers, J. E. Towse, and P. Selvendiran (2010), Mercury dynamics in relation to DOC concentration and quality during high-flow events in three northeastern U.S. streams, *Water Resour. Res.*, *46*, W07522, doi:10.1029/2009WR008351.
- Driscoll, C. T., V. Blette, C. Yan, C. L. Schofield, R. Munson, and J. Holsapple (1995), The role of dissolved organic carbon in the chemistry and bioavailability of mercury in remote Adirondack lakes, *Water Air Soil Pollut.*, *80*(1–4), 499–508.
- Drott, A., L. Lambertsson, E. Björn, and U. Skjällberg (2007), Importance of dissolved neutral mercury sulfides for methyl mercury production in contaminated sediments, *Environ. Sci. Technol.*, *41*(7), 2270–2276.
- Fischer, D. (1957), Bedrock geology map of New York State, *NYS Mus. Bull.*, *221*(4).
- Galloway, M. E., and B. A. Branfireun (2004), Mercury dynamics of a temperate forested wetland, *Sci. Total Environ.*, *325*(1–3), 239–254.
- Grigal, D. F. (2003), Mercury sequestration in forests and peatlands: A review, *J. Environ. Qual.*, *32*(2), 393–405.
- Güntner, A., J. Seibert, and S. Uhlenbrook (2004), Modeling spatial patterns of saturated areas: An evaluation of different terrain indices, *Water Resour. Res.*, *40*, W05114, doi:10.1029/2003WR002864.
- Haitzer, M., G. R. Aiken, and J. N. Ryan (2002), Binding of mercury(II) to dissolved organic matter: The role of the mercury-to-DOM concentration ratio, *Environ. Sci. Technol.*, *36*(16), 3564–3570.
- Hill, A. R. (2000), Stream chemistry and riparian zones, in *Streams and Ground Waters*, edited by J. Jones and P. Mulholland, pp. 84–110, Academic, New York.
- Hornberger, G. M., K. E. Bencala, and D. M. McKnight (1994), Hydrological controls on dissolved organic carbon during snowmelt in the Snake River near Montezuma, Colorado, *Biogeochemistry*, *25*(3), 147–165.
- Ibbitt, R. P., R. A. Woods, and M. P. Clark (2009), Assimilating stream-flow data to update water table positions in rainfall-to-runoff models based on topmodel concepts, *N. Z. J. Hydrol.*, *48*(1), 13–28.
- Inamdar, S. P., and M. J. Mitchell (2006), Hydrologic and topographic controls on storm-event exports of dissolved organic carbon (DOC) and nitrate across catchment scales, *Water Resour. Res.*, *42*, W03421, doi:10.1029/2005WR004212.
- Klaminder, J., R. Bindler, J. Rydberg, and I. Renberg (2008), Is there a chronological record of atmospheric mercury and lead deposition preserved in the mor layer (O-horizon) of boreal forest soils?, *Geochim. Cosmochim. Acta*, *72*(3), 703–712.
- Kolka, R. K., D. F. Grigal, E. A. Nater, and E. S. Verry (2001), Hydrologic cycling of mercury and organic carbon in a forested upland-bog watershed, *Soil Sci. Soc. Am. J.*, *65*(3), 897–905.
- Krabbenhoft, D. P., B. A. Branfireun, and A. Heyes (2005), Biochemical cycles affecting the speciation, fate and transport of mercury in the environment, in *Mercury: Sources, Measurements, Cycles and Effects*, edited by M. B. Pearson and J. B. Percival, pp. 139–156, Mineral. Assoc. of Canada, Quebec, Ont.
- Lewis, M. E., and M. E. Brigham (2004), Low-level mercury (version 1.0), *U.S. Geol. Surv. Tech. Water Resour. Invest.*, book 9, chap. A5, section 5.6.4.B. (Available at http://water.usgs.gov/owq/FieldManual/chapter5/pdf/5.6.4.B_v1.0.pdf, accessed 14 May 2010)
- Lindberg, S., R. Bullock, R. Ebinghaus, D. Engstrom, X. Feng, W. Fitzgerald, N. Pirrone, E. Prestbo, and C. Seigneur (2007), A synthesis of progress and uncertainties in attributing the sources of mercury in deposition, *Ambio*, *36*(1), 19–32.
- McHale, M. R., M. J. Mitchell, J. J. McDonnell, and C. P. Cirno (2000), Nitrogen solutes in an Adirondack forested watershed: Importance of dissolved organic nitrogen, *Biogeochemistry*, *48*(2), 165–184.
- McHale, M. R., J. J. McDonnell, M. J. Mitchell, and C. P. Cirno (2002), A field-based study of soil water and groundwater nitrate release in an Adirondack forested watershed, *Water Resour. Res.*, *38*(4), 1031, doi:10.1029/2000WR000102.
- Mitchell, C. P. J., B. A. Branfireun, and R. K. Kolka (2008a), Total mercury and methylmercury dynamics in upland-peatland watersheds during snowmelt, *Biogeochemistry*, *90*(3), 225–241.
- Mitchell, C. P. J., B. A. Branfireun, and R. K. Kolka (2008b), Assessing sulfate and carbon controls on net methylmercury production in peatlands: An in situ mesocosm approach, *Appl. Geochem.*, *23*(3), 503–518.
- Mitchell, C. P. J., B. A. Branfireun, and R. K. Kolka (2008c), Spatial characteristics of net methylmercury production hot spots in peatlands, *Environ. Sci. Technol.*, *42*(4), 1010–1016.
- Mitchell, M. J., P. J. McHale, S. Inamdar, and D. J. Raynal (2001), Role of within-lake processes and hydrobiogeochemical changes over 16 years in a watershed in the Adirondack Mountains of New York state, USA, *Hydrol. Process.*, *15*(10), 1951–1965.
- Muir, D. C. G., et al. (2009), Spatial trends and historical deposition of mercury in eastern and northern Canada inferred from lake sediment cores, *Environ. Sci. Technol.*, *43*(13), 4802–4809.
- Munthe, J., R. A. Bodaly, B. A. Branfireun, C. T. Driscoll, C. C. Gilmour, R. Harris, M. Horvat, M. Lucotte, and O. Malm (2007), Recovery of mercury-contaminated fisheries, *Ambio*, *36*(1), 33–44.
- Nash, J. E., and J. V. Sutcliffe (1970), River flow forecasting through conceptual models, part 1 – A discussion of principles, *J. Hydrol.*, *10*, 282–290.
- Olson, M. L., and J. F. DeWild (1999), Techniques for the collection and species-specific analysis of low levels of mercury in water, sediment, and biota, 11 pp., *U.S. Geol. Surv. Water Resour. Invest. Rep.*, 99–4018-B.
- Olund, S. D., J. F. DeWild, M. L. Olson, and M. T. Tate (2004), Methods for the preparation and analysis of solids and suspended solids for total mercury, 23 pp., *U.S. Geol. Surv. Tech. Methods Rep.*, 5–A8.
- Pacyna, E. G., J. M. Pacyna, F. Steenhuisen, and S. Wilson (2006), Global anthropogenic mercury emission inventory for 2000, *Atmos. Environ.*, *40*(22), 4048–4063.
- Peters, S. C., J. L. Wollenberg, D. P. Morris, and J. A. Porter (2007), Mercury emission to the atmosphere from experimental manipulation of DOC and UVR in mesoscale field chambers in a freshwater lake, *Environ. Sci. Technol.*, *41*(21), 7356–7362.
- Ramlal, P. S., C. A. Kelly, J. W. M. Rudd, and A. Furutani (1993), Sites of methyl mercury production in remote Canadian Shield lakes, *Can. J. Fish. Aquat. Sci.*, *50*(5), 972–979.
- Schuster, F. P., J. B. Shanley, M. Marvin-Dipasquale, M. M. Reddy, G. R. Aiken, D. A. Roth, H. E. Taylor, D. P. Krabbenhoft, and J. F. DeWild (2008), Mercury and organic carbon dynamics during runoff episodes from a northeastern USA watershed, *Water Air Soil Pollut.*, *187*(1–4), 89–108.
- Seibert, J., and B. L. McGlynn (2007), A new triangular multiple flow direction algorithm for computing upslope areas from gridded digital elevation models, *Water Resour. Res.*, *43*, W04501, doi:10.1029/2006WR005128.
- Selvendiran, P., C. T. Driscoll, J. T. Bushey, and M. R. Montesdeoca (2008), Wetland influence on mercury fate and transport in a temperate forested watershed, *Environ. Pollut.*, *154*(1), 46–55.
- Selvendiran, P., C. T. Driscoll, M. R. Montesdeoca, H. D. Choi, and T. M. Holsen (2009), Mercury dynamics and transport in two Adirondack lakes, *Limnol. Oceanogr.*, *54*(2), 413–427.
- Shanley, J. B., C. Kendall, T. E. Smith, D. M. Wolock, and J. J. McDonnell (2002), Controls on old and new water contributions to stream flow at some nested catchments in Vermont, USA, *Hydrol. Process.*, *16*(3), 589–609.
- Shanley, J. B., et al. (2008), Comparison of total mercury and methylmercury cycling at five sites using the small watershed approach, *Environ. Pollut.*, *154*(1), 143–154.

- Shepard, J. P., M. J. Mitchell, T. J. Scott, Y. M. Zhang, and D. J. Raynal (1989), Measurements of wet and dry deposition in a northern hardwood forest, *Water Air Soil Pollut.*, 48(1-2), 225-238.
- Ullrich, S. M., T. W. Tanton, and S. A. Abdrashitova (2001), Mercury in the aquatic environment: A review of factors affecting methylation, *Crit. Rev. Environ. Sci. Technol.*, 31(3), 241-293.
- U.S. Environmental Protection Agency (EPA) (1996), Method 1669, sampling ambient water for trace metals at EPA water quality criteria levels, 35 pp., Washington, D. C.
- U.S. Environmental Protection Agency (EPA) (2009), 2008 biennial listing of fish advisories, *U.S. Environ. Prot. Agency Rep. EPA-823-F-09-007*, 7 pp., Washington, D. C.
- van Verseveld, W. J., J. J. McDonnell, and K. Lajtha (2008), A mechanistic assessment of nutrient flushing at the catchment scale, *J. Hydrol.*, 358(3-4), 268-287.
- Weiler, M., and J. McDonnell (2004), Virtual experiments: A new approach for improving process conceptualization in hillslope hydrology, *J. Hydrol.*, 285(1-4), 3-18.
- Weiler, M., and J. R. J. McDonnell (2006), Testing nutrient flushing hypotheses at the hillslope scale: A virtual experiment approach, *J. Hydrol.*, 319(1-4), 339-356.
- Weishaar, J. L., G. R. Aiken, B. A. Bergamaschi, M. S. Fram, R. Fujii, and K. Mopper (2003), Evaluation of specific ultraviolet absorbance as an indicator of the chemical composition and reactivity of dissolved organic carbon, *Environ. Sci. Technol.*, 37(20), 4702-4708.
- Wetzel, R. G., P. G. Hatcher, and T. S. Bianchi (1995), Natural photolysis by ultraviolet irradiance of recalcitrant dissolved organic matter to simple substrates for rapid bacterial metabolism, *Limnol. Oceanogr.*, 40(8), 1369-1380.
- Wiener, J. G., B. C. Knights, M. B. Sandheinrich, J. D. Jeremiason, M. E. Brigham, D. R. Engstrom, L. G. Woodruff, W. F. Cannon, and S. J. Balogh (2006), Mercury in soils, lakes, and fish in Voyageurs National Park (Minnesota): Importance of atmospheric deposition and ecosystem factors, *Environ. Sci. Technol.*, 40(20), 6261-6268.
- Wolock, D. M. (1993), Simulating the variable-source-area concept of watershed hydrology with TOPMODEL, *U.S. Geol. Surv. Water Resour. Invest. Rep.*, 93-4124, 33.
-
- D. A. Burns, Watersheds Research Section, U.S. Geological Survey, 425 Jordan Rd., Troy, NY 12180-8349, USA.
- H. Laudon and J. Schelker, Department of Forest Ecology and Management, Swedish University of Agricultural Sciences, SE-901 83 Umeå, Sweden. (jakob.schelker@slu.se)
- M. Weiler, Institute of Hydrology, Albert-Ludwigs-Universität Freiburg, Fahnbergplatz, D-79085 Freiburg, Germany.